Journal of Biomedical Optics

SPIEDigitalLibrary.org/jbo

Singlet gradient index lens for deep *in vivo* multiphoton microscopy

Teresa A. Murray
Michael J. Levene

SPIE

Singlet gradient index lens for deep *in vivo* multiphoton microscopy

Teresa A. Murray[a,b] and Michael J. Levene[a]
[a]Yale University, Department of Biomedical Engineering, New Haven, Connecticut 06511
[b]Louisiana Tech University, Center for Biomedical Engineering and Rehabilitation Science, Ruston, Louisiana 71270

Abstract. Micro-optical probes, including gradient index (GRIN) lenses and microprisms, have expanded the range of *in vivo* multiphoton microscopy to reach previously inaccessible deep brain structures such as deep cortical layers and the underlying hippocampus in mice. Yet imaging with GRIN lenses has been fundamentally limited by large amounts of spherical aberration and the need to construct compound lenses that limit the field-of-view. Here, we demonstrate the use of 0.5-mm-diameter, 1.7-mm-long GRIN lens singlets with 0.6 numerical aperture in conjunction with a cover glass and a conventional microscope objective correction collar to balance spherical aberrations. The resulting system achieves a lateral resolution of 618 nm and an axial resolution of 5.5 μm, compared to lateral and axial resolutions of ~1 μm and ~15 μm, respectively, for compound GRIN lenses of similar diameter. Furthermore, the GRIN lens singlets display fields-of-view in excess of 150 μm, compared with a few tens of microns for compound GRIN lenses. The GRIN lens/cover glass combination presented here is easy to assemble and inexpensive enough for use as a disposable device, enabling ready adoption by the neuroscience community. [DOI: 10.1117/1.JBO.17.2.021106]

Keywords: multiphoton microscopy; fluorescence; GRIN lens; aberrations; hippocampus; in vivo.

Paper 11520SS received Sep. 24, 2011; revised manuscript received Nov. 4, 2011; accepted for publication Nov. 7, 2011; published online Mar. 2, 2012.

1 Introduction

Multiphoton microscopy (MPM) has become the tool of choice for *in vivo* fluorescence imaging due to its superior penetration depth through scattering tissue. Although recent work using cortical excavation,[1,2] regenerative amplifiers,[3] or very long wavelength laser[4] sources have sought to extend the maximum imaging depth of MPM up to ~1-mm, routine MPM in mouse brain is typically limited to a few hundred microns. Micro-optics, including both gradient index (GRIN) lenses[5,6] and microprisms,[7,8] have extended the range of conventional MPM microscopes up to several millimeters. Most GRIN lenses used for MPM have been compound lenses in which a high (0.5 to 0.6) numerical aperture (NA) objective of less than 1/4 pitch is glued to a lower-NA (0.1) relay lens. This is necessary in order to avoid focusing the short-pulse excitation laser inside the higher-NA material, which can result in bright fluorescence from the lens. However, this reduces the field-of-view by the ratio of the NAs of the relay and objective lenses (e.g., by 1/6 for a 0.6 NA objective with a 0.1 NA relay). In addition, GRIN lenses suffer from severe optical aberrations, most significantly distortion and spherical aberration. While distortion acts to further limit the effective field-of-view, spherical aberration severely degrades the image quality. Early compound GRIN lenses for MPM had lateral resolutions of ~1 μm and axial resolutions as low as 12 to 15 μm.[5,6] Recently, a compound lens consisting of a plano-convex, 0.8-NA objective lens coupled to a 0.45-NA GRIN relay lens has been shown to improve spherical aberration, with 1 μm lateral resolution and 4.4 μm axial resolution.[9,10] This system has an outer diameter, including the metal sheath that contains the lens assembly, of 1.4 mm and therefore requires the removal of a significant amount of brain tissue over the region to be imaged. In addition, they are fairly expensive for a disposable device.

In general, aberrations from GRIN lenses scale with pitch length, such that using shorter lenses results in reduced aberrations. Nonetheless, even using GRIN lenses slightly less than 1/2 pitch can result in significant positive spherical aberration. Correction collars on commercial objective lenses typically add more positive spherical aberration to correct for the negative aberration induced by cover glasses, and therefore cannot be used alone to compensate for aberrations in GRIN lenses. However, we show here that a cover glass placed between the objective and a short GRIN lens can be used to compensate for the aberrations in the GRIN lens, with the correction collar of the objective used to rebalance any overcompensation by the cover glass. In addition, the system we present here is compact, easily integrated into standard MPM microscopes, and relatively inexpensive.

2 Methods

The homebuilt multiphoton microscope has been previously described[11,12] with the exception that the laser power was modulated by a Pockels cell (Model 350-80-LA-02 with a Model 302RM driver, ConOptics, Danbury, CT), and a 1-meter effective focal length lens was used to reduce the amount of overfilling of the back aperture, maximizing the laser power through the objective. Briefly, the microscope system was composed of a MaiTai Ti:sapphire mode-locked laser (Spectra-Physics, Mountain View, CA), a homebuilt microscope based on a BX51 upright microscope (Olympus America, Center Valley, PA) with homebuilt filter and detector housing, and an HC-125-02 photomultiplier tube (PMT; Hamamatsu Corporation,

Address all correspondence to: Michael J. Levene, Yale University, Department of Biomedical Engineering, New Haven, Connecticut 06511. Tel: (203) 432-4264; Fax: (203) 432-0030; E-mail: michael.levene@yale.edu

0091-3286/2012/$25.00 © 2012 SPIE

Bridgewater, NJ). We used a LUCPlanFLN 40X/0.6 NA objective with a correction collar for up to 2 mm of glass (Olympus America), a P-725.4-CD PIFOC QuickLock microscope objective piezoelectric translator with a E-665.CR controller (Physik Instruments GmbH & Co., Karlsruhe, Germany) for adjusting the vertical position of the objective, and an ASI M-2000 motorized stage (Applied Scientific Instruments, Inc., Eugene, OR) for positioning specimens under the lens. Scanning and image acquisition were controlled by ScanImage software.[13]

Positioning the GRIN lens assembly under the microscope objective was facilitated by a custom built lens holder bolted to the underside of the microscope nosepiece [Fig. 1(a)]. Our lens positioner was composed of a three-axis micromanipulator, a 2" kinetic platform mount with two tilt axes (Model KM100B, Thorlabs, Newton, NJ), and a machined aluminum arm with a GRIN lens mounting device [Fig. 1(b)]. A small steel mounting plate with a 3-mm clear aperture held the magnet on the GRIN lens assembly.

Each of our GRIN lens assemblies consisted of a 500-μm-diameter GRIN lens, a small glass cover slip, and a magnetic washer [Fig. 1(b)]. GRIN lenses were supplied by GoFoton with specifications, as follows: 500-μm diameter ILH uncoated GRIN lens, 0.6NA, just under 1/2 pitch, 150-μm working distance in glass at one end and 150-μm in water at the other end. The length of each lens was 1.689 mm. A cleaned #1.5 glass cover slip (Harvard Apparatus, Holliston, Massachusetts, USA), which is 170 μm thick, was glued to one end of the GRIN lens with Norland No. 73 optical adhesive (Norland Products, Inc., Cranbury, NJ) to partly compensate for spherical aberration inherent in GRIN lenses. Nickel-plated neodymium washers measuring $0.5''\text{OD} \times 0.25''\text{ID} \times 0.031''$ thick (K&J Magnetics, Inc., www.kjmagnetics.com) were glued to the cover slips with Norland No. 73 optical adhesive (Norland Products, Inc., Cranbury, NJ). Using a magnet simplifies the design of the holding apparatus and results in a secure hold. An additional 1-mm cover glass was placed on top of the lens holder to provide additional negative spherical aberration.

We characterized the point spread function (PSF) of our GRIN lens system using the second harmonic (SHG) signal from 100-nm barium titanate ($BaTiO_3$) nanoparticles (Sigma-Aldrich Corp, St. Louis, MO) incorporated into 2% agarose gel. Unlike fluorescent particles normally used for PSF measurements, SHG from $BaTiO_3$ particles does not photobleach and does not saturate. The SHG was collected using 886-nm laser excitation and a 430/100-nm band-pass filter (HQ430/100M-2P, Chroma Technology Corp., Rockingham, VT). A z-stack was acquired using the piezo translator to move the objective in either 0.5- or 1-μm steps. A custom MATLAB program was used to calculate the full-width-at-half-maximum (FWHM) for the lateral and axial directions from a z-stack containing a single nanoparticle. PSF measurements were acquired for the $40\times/0.6$ NA objective alone and coupled to either a GRIN lens without a cover slip or one with a cover slip attached and a 1-mm-thick piece of glass placed above the GRIN lens assembly. Measurements were taken of particles within the central 50% of the GRIN lens field-of-view. The optimal correction collar setting was determined empirically as the setting that produced the smallest PSF.

For *in vivo* imaging, a GRIN lens was inserted into the cortex of a Thy1-YFPH transgenic mouse[14] through a craniotomy, as previously described[8] with a few exceptions as follows. All craniotomies were 2 mm posterior to bregma and 1 mm lateral to the midline. A 30-gauge needle was used to pierce and remove the dura, and sterile, physiological saline was applied to the craniotomy to keep the brain tissue hydrated. A blunted 23-gauge hypodermic needle was used to aspirate a column of cortical tissue without penetrating the corpus callosum. Aspiration was accomplished in stages beginning with advancing the needle tip 100 to 200 μm and then retracting the needle, irrigating the cavity with sterile saline, waiting for bleeding to stop, and then aspirating the fluid. More saline was applied if bleeding had not stopped. This procedure was repeated until a depth of 800 μm was reached. Once the bleeding was controlled and residual blood removed, the cavity was filled with sterile saline.

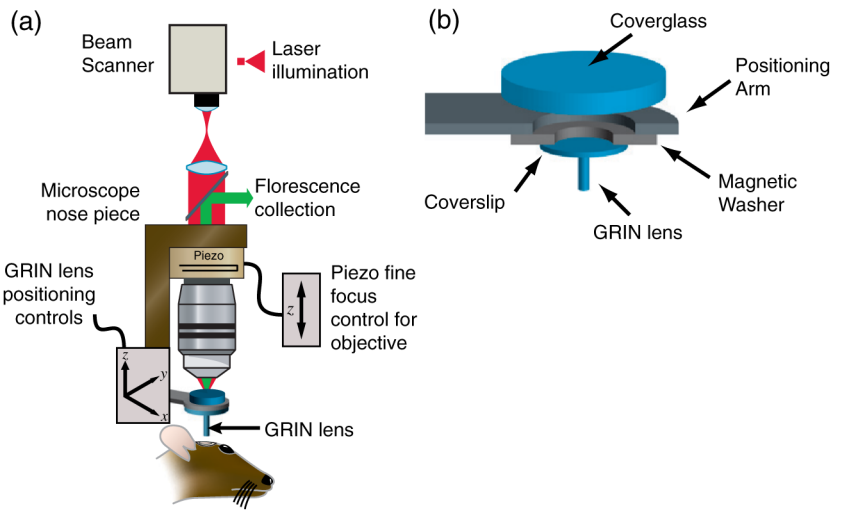

Fig. 1 GRIN lens positioning apparatus. (a) Three-axis controls for positioning of the GRIN lens relative to the microscope objective are attached to the microscope nosepiece. A piezo element enables fine focus control without moving the GRIN lens after it is inserted into tissue. (b) The GRIN lens is attached to a cover slip that contributes negative spherical aberration to balance the positive spherical aberration of the lens. The cover slip is glued to a magnetic washer for easy attachment and removal from the positioning arm (washer and arm shown here as cutaways). An additional, 1-mm-thick cover glass is placed on top of the positioning arm contributes additional negative spherical aberration.

All procedures involving mice were in accordance with protocols approved by the Yale Institutional Animal Care and Use Committee.

For imaging, the anesthetized mouse was transferred in a surgical frame to the microscope stage under the prealigned GRIN lens. The stage was periodically moved up, and images were taken at each position until the desired depth was reached as evidenced by the appearance of fluorescently labeled pyramidal cells in the hippocampus. After reaching the desired implant depth, the piezo translator was used to change the plane of focus without moving the lens in the brain tissue. Images of neurons expressing YFP were acquired using 886-nm laser excitation and a 535-nm/50-nm band-pass filter (ET535/50M-2P, Chroma Technology Co.).

3 Results and Discussion

Lateral and axial resolutions were compared between our optimized system and a nonoptimized system. Our optimized system included a GRIN lens with a glass cover slip attached and an additional 1-mm-thick cover glass placed between the microscope objective and GRIN lens. Our nonoptimized condition used an unmodified GRIN lens. Both the lateral and axial PSF were markedly smaller for our optimized configuration (Fig. 2). A diffraction-limited PSF would result in lateral and axial FWHMs of 556 nm and 3.99 μm, respectively. For the nonoptimized condition, the lateral and axial FWHM measurements had mean $\pm$ s.e.m. of 782 ± 58 nm and 14.313 ± 0.351 μm ($n = 3$), respectively, corresponding to 141% and 359% of the diffraction limit. In contrast, the lateral and axial FWHM values for our optimized system were 618 ± 5 nm and 5.537 ± 0.085 μm ($n = 4$), respectively, corresponding to 111% and 139% of the diffraction limit. For comparison, previously published results using a compound GRIN lens with a 0.8 NA plano-convex lens and 920 nm excitation resulted in PSFs with lateral and axial FWHM values of 606 nm and 2.8 μm, respectively, corresponding to 140% and 130% of the diffraction limit.

Spherical aberration results in much greater broadening of the axial PSF than the lateral PSF. Given the ratio of axial:lateral FWHM for the optimized system, the residual deviation from diffraction-limited performance is likely due to coma, perhaps due in part to a small tilt of the GRIN lens relative to the optical axis. Chromatic aberration is not expected to have a large impact for multiphoton microscopy because the bandwidth of the excitation pulse is only ~10 nm, and the fluorescence signal is collected by large-area, nondescanned detectors.

In vivo imaging of neurons in mouse hippocampus demonstrates the resolution of the GRIN lens assemblies.

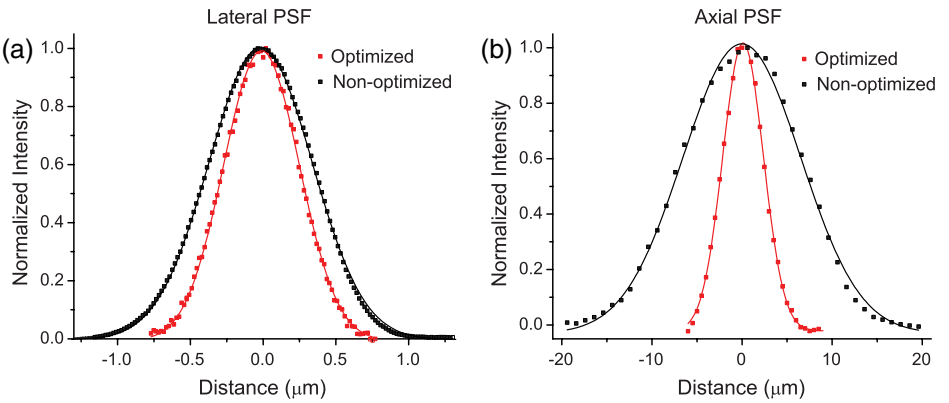

Fig. 2 Sample multiphoton PSFs of optimized and nonoptimized GRIN lenses. (a) GRIN lenses optimized with aberration-balancing cover slips had lateral PSF FWHMs of 618 ± 5 nm compared to nonoptimized singlets with FWHMs of 782 ± 58 nm. (b) Axial PSF FWHMs were 5.537 ± 0.085 μm for the optimized system compared to 14.313 ± 0.351 μm for GRIN singlets.

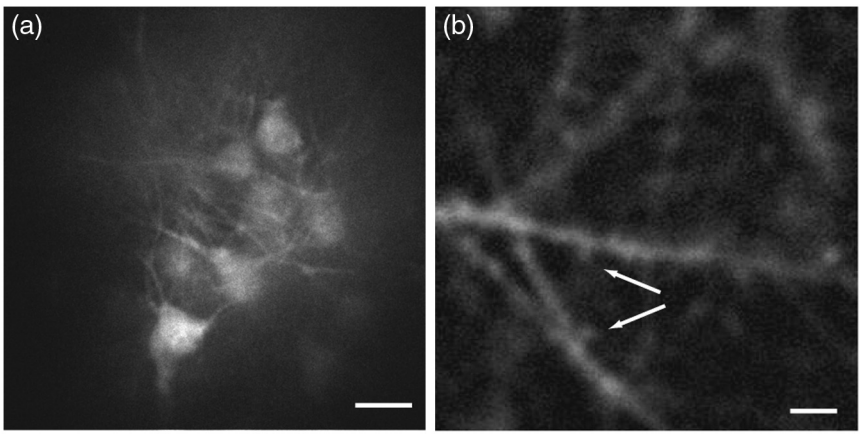

Fig. 3 *In vivo* multiphoton microscopy of hippocampus in Thy1-YFP line H mice with optimized GRIN lens system. (a) Individual cell bodies and fine processes are clearly visible within a 200 μm field-of-view. (b) Resolution is sufficient to identify spines on fine processes (white arrows). Scale bars are (a) 30 μm and (b) 2 μm.

The 1.689-mm length of these lenses allows imaging of the hippocampus of mice with a lens assembly that is nearly flush with the skull of a mouse. Representative images of CA1 hippocampal neurons [Fig. 3(a)] and processes [Fig. 3(b)] show excellent resolution. As shown in Fig. 3a, the effective field-of-view is $>120\ \mu$m. The fluorescence intensity rolls off near the edges of the field-of-view due to increased off-axis aberrations and decreases in the effective numerical aperture. Previously, compound GRIN lenses used for MPM with 0.5 mm or smaller diameter have been limited to a field-of-view of only a few tens of microns.[5,6] Moreover, we were able to resolve the presence of large dendritic spines in our images [Fig. 3(b), arrows].

4 Conclusions

In summary, compared to previous compound lenses with similar diameters, combining a short GRIN lens singlet with a cover glass and a correction collar for balancing spherical aberration has improved the lateral resolution almost twofold and the axial resolution almost threefold. The field-of-view is also improved by more than threefold. Although recent commercially available compound lenses using plano-convex objectives have achieved higher resolution, the simple system presented here comes closer to diffraction-limited performance, albeit with a lower NA. Furthermore, the markedly smaller diameter of these lenses results in ~87% less tissue displacement. In addition, the overall cost of the lens assemblies at the present time is 1/10 of the cost of the commercially available compound lenses, making them essentially disposable lenses.

Acknowledgments

Funding for this work was provided by NSF CAREER Award DBI-0953902. We express our appreciation to Thomas Chia, Joseph Zinter, Nathan Gilfoy, and Amanda Foust (Yale University, New Haven, CT) for technical assistance.

References

1. A. Mizrahi et al., "High-resolution in vivo imaging of hippocampal dendrites and spines," *J. Neurosci.* **24**(13), 3147–3151 (2004).
2. D. A. Dombeck et al., "Functional imaging of hippocampal place cells at cellular resolution during virtual navigation," *Nat. Neurosci.* **13**(11), 1433–1440 (2010).
3. P. Theer, M. T. Hasan, and W. Denk, "Two-photon imaging to a depth of 1000 μm in living brains by use of a $Ti:Al_2O_3$ regenerative amplifier," *Opt. Lett.* **28**(12), 1022–1024 (2003).
4. D. Kobat et al., "Deep tissue multiphoton microscopy using longer wavelength excitation," *Opt. Express* **17**(16), 13354–13364 (2009).
5. M. J. Levene et al., "In vivo multiphoton microscopy of deep brain tissue," *J. Neurophys.* **91**(5), 1908–1912 (2004).
6. J. C. Jung et al., "In vivo mammalian brain imaging using one- and two-photon fluorescence microendoscopy," *J. Neurophys.* **92**(5), 3121–3133 (2004).
7. T. H. Chia and M. J. Levene, "Microprisms for in vivo multilayer cortical imaging," *J. Neurophys.* **102**(2), 1310–1314 (2009).
8. T. H. Chia and M. J. Levene, "In vivo imaging of deep cortical layers using a microprism," *J. Visual. Exp.* (2009) (www.jove.com/index/Details.stp?ID=1509) [DOI: 10.3791/1509].
9. R. P. J. Barretto, B. Messerschmidt, and M. J. Schnitzer, "In vivo fluorescence imaging with high-resolution microlenses," *Nat. Methods* **6**(7), 511–561 (2009).
10. B. Messerschmidt et al., "Novel concept of GRIN optical systems for high resolution microendoscopy. Part 1: Physical aspects," *Proc SPIE*, **6432**, 643202 (2007).
11. T. H. Chia et al., "Multiphoton fluorescence lifetime imaging of intrinsic fluorescence in human and rat brain tissue reveals spatially distinct NADH binding," *Opt. Express* **16**(6), 4237–4249 (2008).
12. J. P. Zinter and M. J. Levene, "Maximizing fluorescence collection efficiency in multiphoton microscopy," *Opt. Express* **19**(16), 15348–15362 (2011).
13. T. A. Pologruto, "Monitoring neural activity and [Ca2+] with genetically encoded Ca2+ indicators," *J. Neurosci.* **24**(43), 9572–9579 (2004).
14. G. Feng et al., "Imaging neuronal subsets in transgenic mice expressing multiple spectral variants of GFP," *Neuron* **28**(1), 41–51 (2000).